Journal of Cellular Biochemistry 97:544–552 (2006)

Structure and Growth of Ultrasmall Protein Microcrystals by Synchrotron Radiation: I. μGISAXS and μDiffraction of P450scc

Claudio Nicolini[1,2]* and Eugenia Pechkova[1,2]

[1]Fondazione EL.B.A., via delle Testuggini snc, 00187 Roma, Italy
[2]Nanoworld Institute and Biophysics Division, University of Genoa, Corso Europa 30, 16132 Genoa, Italy

Abstract Ultrasmall P450scc cytochrome microcrystals are grown by classical hanging vapor diffusion and by its modification using homologous protein thin-film template displaying a long-range order. The nucleation and growth mechanisms of P450scc microcrystals are studied at the thin cytochrome film surface by a new microbeam grazing incidence small angle X-ray scattering (μGISAXS) technique developed at the microfocus beamline of the European Synchrotron Radiation Facility (ESRF) in Grenoble, France. P450scc cytochrome crystals of about 5 μm are also investigated by synchrotron radiation diffraction in order to attempt a preliminary analysis of the atomic structure of this unique protein system yet unsolved. J. Cell. Biochem. 97: 544–552, 2006. © 2005 Wiley-Liss, Inc.

Key words: synchrotron scattering diffraction; P450scc microcrystals; microbeam grazing incidence

The techniques of elastic scattering of X-rays are widely used as they provide valuable tools to probe the order properties of protein crystals. The diffraction range is reached when the incident radiation wavelength is closed to the interatomic distances in a crystal and when the scattering angles are wide. By a careful analysis of the integrated diffracted intensities, one can access to the intimate atomic structure, that is, the positions of nuclei and the spread of the electronic cloud around atoms [Guinier and Fournet, 1955; Guinier, 1963]. The range of "diffuse scattering" involves instead techniques, which allow getting statistical information at scales that are greater than the interatomic distances [Gehrke, 1992; Holy and Baumbach, 1994]. This domain is restricted in between the first Bragg peak, which overlaps with the direct beam and the diffraction peaks [Guinier and Fournet, 1955; Guinier, 1963], useful to determine the atomic structure of protein crystal [Guinier, 1963; Pechkova and Nicolini, 2003]. With X-rays with a wavelength of a few angstroms, this domain of small momentum transfer is reached in the small angle range [Gehrke, 1992; Holy and Baumbach, 1994; Müller-Buschbaum et al., 1998]. The scattering comes from strong variations of the mean electronic density for X-rays and up to 15 years ago was limited to three dimensional samples as the strong penetration depth of the radiations and the low signal to noise ratio hampered the surface sensitivity. Quite recently, thanks to highly focused synchrotron radiation [Riekel, 2000], these techniques were extended to surface geometry using the phenomenon of total reflection of X-rays in the grazing incidence range [Müller-Buschbaum et al., 2003]. The field of thin films growth brought a need of knowledge about layer morphology and sizes of quantum dots, supported islands or buried particles, which has pushed down to the micrometer size for incoming beam the development of grazing incidence small angle X-ray scattering (μGISAXS) [Müller-Buschbaum et al., 2000, 2003; Roth et al., 2003], providing information at the highest sensitivity down to the nanometer scale

Grant sponsor: FIRB-MIUR.

*Correspondence to: Claudio Nicolini, Nanoworld Institute and Biophysics Division, University of Genoa, Corso Europa 30, 16132 Genoa, Italy.
E-mail: manuscript@ibf.unige.it

Received 10 January 2005; Accepted 28 April 2005
DOI 10.1002/jcb.20537

© 2005 Wiley-Liss, Inc.

for the dependence of the electronic density perpendicular to the surface, like those due to the roughness of a surface, the lateral correlations, sizes and shapes of gold nanoparticles [Roth et al., 2003]. Such information are of prime interest in understanding the link between growing ultrasmall crystal morphology and its physical, chemical, structural properties, the latter being also object of this work down to atomic resolution by X-ray microfocus diffraction [Riekel, 2000].

For understanding the basic physical aspects of the template induced P450scc cytochrome microcrystal nucleation and growth, the synchrotron microfocus has being here used both for diffraction and μGISAXS experiments [Lazzari, 2002; Roth et al., 2003; Nicolini and Pechkova, 2004].

As scanning force microscopy (SFM), sensitive only to surface structures, GISAXS appears an excellently suited method for structural and morphological studies of patterned thin films [Müller-Buschbaum et al., 1998, 2000] and of cytochromes P450scc crystal growth and nucleation at its very early stages, as induced by classical [Ducruix and Giege, 1999] and nanotemplate-based [Pechkova and Nicolini, 2002a,b] vapor diffusion method.

MATERIALS AND METHODS

Protein and Chemicals

The expression vector pTrc99A was purchased from Pharmacia Biotech. Restriction enzymes were obtained from Boehringer-Mannheim (Milan, Italy). Reagents for bacterial growth were from Fluka (Buchs, Switzerland). Emulgen 913 was kindly provided by Kao Chemical (Tokyo, Japan).

Protein molecular weight standards were from Promega. Hydroxyapatite column was from BioRad (Milan, Italy). Other chemicals were purchased from Sigma Aldrich (Milan, Italy).

Expression and Purification of Recombinant Native P450scc in *E. coli*

JM109 cells, transformed with pTrc99A-P450scc expression plasmid, were grown and induced as described in Wada et al. [1991] with following modifications: (-aminolevulinic acid (1 mM), a precursor of heme biosynthesis, was added at the same time as isopropyl-1-thio-β-D-galactopyranoside (1 mM) and the cells were grown for 72 h at 28°C by shaking at 150 rpm.

Expressed cytochrome P450scc was purified by three different chromatographic steps: DEAE cellulose, hydroxyapatite, and Adx-sepharose 4B columns. The sample was solubilized in 10 mM K phosphate buffer (pH 7.4) containing 0.1 mM EDTA, 0.2 sodium cholate, and 20% glycerol and stored at −80°C.

Homologous Nanobiofilm Template

The innovative crystallization method is described in [Pechkova and Nicolini, 2002a,b]. The protein thin-film nanotemplate is created using Langmuir–Schaeffer (LS) technology or modifications of it, and is subsequently deposited on a solid glass support, to be placed in the appropriate vapor-diffusion apparatus, used in the traditional hanging drop vapor-diffusion method. This LS cytochrome P450scc thin film assumes the role of the template for P450scc nucleation and crystal growth. In every drop protein solution pH 7.4, 1M NaCl, 0.3 NaColate is mixed in proportion (1:1) with precipitating buffer pH 7.4, 0.1M $(NH_4)_2SO_4$, 20% PEG 400. Further details on the parameters of the P450scc microcrystal growth are provided in the accompanying study [Pechkova and Nicolini, 2002a,b, 2005].

Moreover, this method seems to produce the more radiation stable crystals, than those obtained by classical techniques [Pechkova et al., 2004]. This aspect concerns also the crystal of miniscule thickness dimensions (5–20 μm) such as the human kinase crystal used for its 3-D structure determination by diffraction using synchrotron microfocus beam [Pechkova and Nicolini, 2003].

X-Ray Microbeam Diffraction

Miniscule P450scc crystals of only a few microns in size, previously unusable for structural analysis, has been used for the collection of diffraction data by third generation synchrotrons, as a result of the introduction of the microfocus beamline [Riekel, 2000]. The Microfocus beamline of the European synchrotron radiation in Grenoble is indeed utilized to probe for the structure of this unique protein system, such as P450scc cytochromes that has remained unsolved until now. The experimental set up here utilized for acquiring the X-ray diffraction patterns is described in Pechkova and Nicolini, 2003.

Microbeam Grazing Incidence X-Ray Scattering

In a grazing incidence experiment (Fig. 1), a monochromatic beam of 5 μm diameter and of wavevector in the X-ray range (wavelength λ) is sent with an incident angle α_i in the range of about 1° onto a surface formed by a protein solution drop containing precipitant and sitting on the homologous protein thin film. The optical elements used for the microbeam preparation and the detector used are described in Roth et al., 2003 and Pechkova et al., 2005.

The layout of the scattering measurements using the reference cartesian frame, which has its origin on the surface and is defined by its z-axis pointing upwards, its x-axis perpendicular to the detector plane and its y-axis along it (Fig. 1). The light is scattered by any type of roughness on the surface. Because of energy conservation, the scattering wave vector **q** is the central quantity (A) to be monitored during the measurements. As shown by Roth et al., 2003 the q_y-dependence (out-of-plane scans) reflects the structure and morphology parallel to the sample surface plane (distances D, in-plane radius R) while the q_z-dependence (detector scans) reflects the height H of clusters, or the roughness parallel to sample surface with:

$$q_y = 2\pi/\lambda \sin(2\theta) \cos(\alpha_f)$$

$$q_z = 2\pi/\lambda \sin(\alpha_i + \alpha_f)$$

As shown in the Figure 1 the scattering intensity is recorded on a plane ensuring that the angles are in the few degrees range and thus enabling the study of lateral sizes of a few nanometers. The direct beam is here suppressed by a beam stop to avoid the detector saturation as several orders of magnitude in intensity separate the diffuse scattering from the reflected beam. The protein solution droplets were placed in the hanging drop container during the 3-day experiment. The glass substrate with the thin film template and the droplet was removed from the container and the vacuum grease area was cleaned to ensure no contamination of the signal. The 10 μl droplet exists for about 60 min in air until complete evaporation since the glass substrate and the atmosphere were both cooled. Hence an optimum timing had to be found concerning the preparation, adjustment in the beam and data acquisition time. The glass

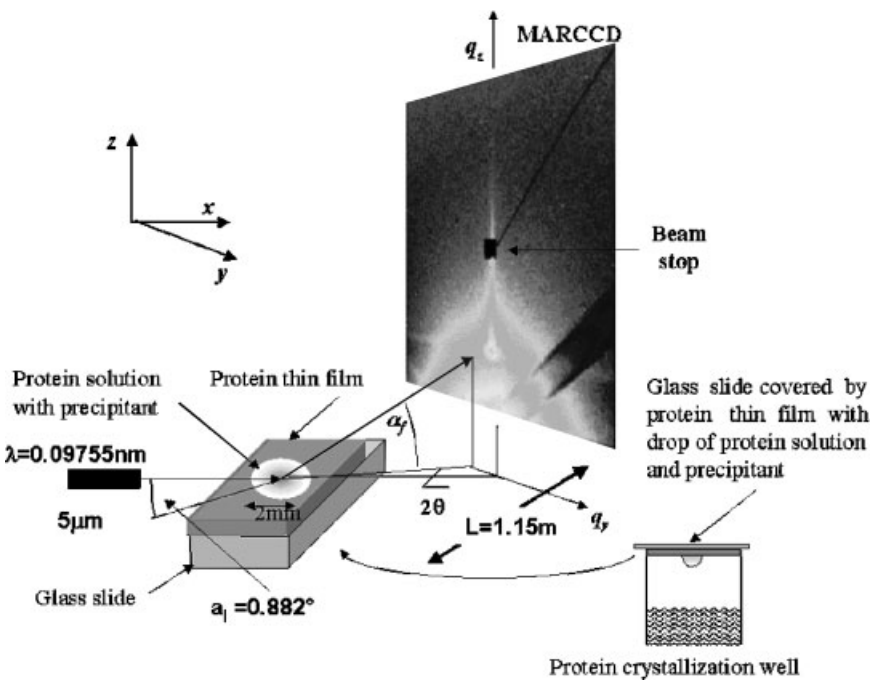

Fig. 1. Schematic view of the microbeam grazing incidence small-angle X-ray scattering setup (μGISAXS) at ID13/ESRF. The sample is mounted on a xyz-gantry and a two-axis goniometer (ϕ_x, ϕ_y). The scan direction is y. α_i denotes the angle between the incident beam and the sample surface, α_f the corresponding exit angle, and 2ϕ the out-of-plane angle. The flight path (L = 1.15 m) between sample and the 2-D detector (C) is evacuated (10^{-2} mbar). The typical 2-D μGISAXS signal of the cytochrome P450scc drop sitting on a layer is also shown. On the bottom right corner it is shown the experimental layout of the protein solution typical droplet sitting on the protein layer deposited over the glass.

substrate was subsequently brought into the beam and the incident angle α_i adjusted to about 1°. This procedure was restricted to less than 20 min in order to avoid precipitation of salt or nanocrystals from the solution to the substrate, which would lead to a contamination of the μGISAXS signal.

A characteristic feature of a GISAXS pattern is the Yoneda peak (Y) [Yoneda, 1963]. This peak occurs at angles $\alpha_i, \alpha_f = \alpha_c$, where α_c is the critical angle of the sample. The critical angle depends on the material via the real part of the refractive index and hence on the density and roughness of the layer over the glass substrate. The relative intensities of the Yoneda peaks can hence be interpreted in terms of build-up over the glass substrate of protein crystal layers, islands of salts and protein crystals and/or of holes in the protein films.

The 10 μl droplet diameter was about 5 mm. Hence the footprint of the X-ray beam will be fully within the droplet diameter. The small beam size allows avoiding excessive liquid scattering and provides therefore a reasonable signal-to-background ratio. The position of the drop relative to the beam was determined by an absorption scan with a photodiode. Experiments were performed with the beam at the center of the droplet at the contact area droplet—protein template in order to optimize the signal of the weakly scattering biopolymer samples. Data collection times for individual droplets varied from 7 to 20 min. This is well below minimum droplet evaporation time of about 60 min. This "Stop" procedure described above interrupts therefore crystal growth at specific times and allows studying microcrystals freshly grown over thin films. The full description of the μGISAXS method is contained in the study coauthored with the Grenoble beamline scientists [Pechkova et al., 2005]. The quoted study is one of a series of studies dealing with the same set-up, and it is the first one describing the experimental details sufficiently. Besides the technical details, the conclusions, results are not derived here and there on a level of the available theory of surface scattering. Several methods of interpreting the data are indeed only mentioned, but not implemented because of the extreme difficulty in utilizing ab initio considerations at the present stage of development. The interpretations was stopped there simply in showing images of the Yoneda peak, while here continue in more depth with in- and out-of- planes data being presented and discussed in both cytochrome (this study) and lysozyme [accompanying study by Pechkova and Nicolini, 2005].

RESULTS

The 2-D scattering patterns (Fig. 1) of q_z, (detector scan) versus q_y (out-of-plane scan) allow to evaluate features like micrystal cluster diameters, heights and distances for the P450scc cytochromes grown either by the nanotemplate-assisted method or the classical one.

μGISAXS measurements of ten layers of P450scc cytochrome being here used as substrate for the subsequent deposition and measurements of crystallizing drop point to the existence of a long range order by plotting the logarithmic signal of intensity versus the q_y (not shown).

Figure 2 shows the clear effect due to the P450scc nanocrystal being formed in the droplet at 44 h after plating and sedimenting over the above P450scc multilayer. Interestingly, while the lower peak in the Yoneda region (Fig. 2B) appears to increase in magnitude with increasing acquisition time, the lower peak in the overall diffuse scattering region (likely corresponding the solution scattering) is drastically decreasing during the same time interval (Fig. 2A).

The effect of sedimentation appears quite different in the droplet containing both buffer and proteins with respect to the one containing only buffer but without proteins: in the latter case the scattering signal is lacking in the lower region even before sedimentation (not shown).

The raw μGISAX patterns of three different drops deposited over the same ten LS layers of P450scc exemplify in Figure 3 the kinetics of protein crystallization in the nanotemplate method versus the classical one (not giving any signal), the role of buffer (not giving any signal) and of thin solid film (giving a signal) in the observed scattering profile.

In summary, under the same conditions of buffer solution and temperature, the μGISAXS images of the 10 μl drop over ten layers of P450scc acting as substrate display the following features:

- lacks any peak and appears quite less intense with diffuse very low scattering signal at the critical angle of the substrate, when it contains only buffer solution with

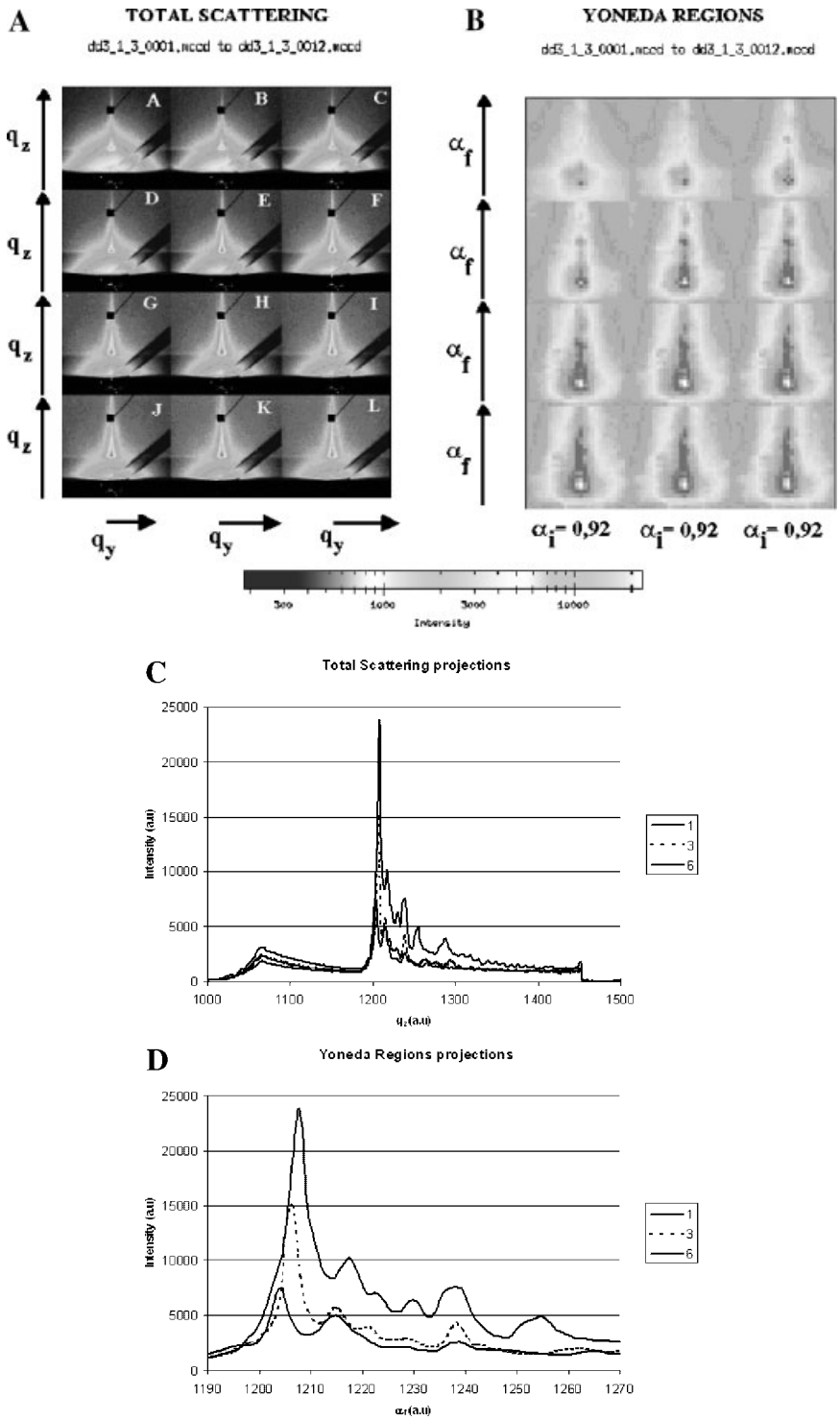

Fig. 2. Raw μGISAXS patterns of a P450scc crystallizing drop sitting over one monolayer of homologous P450 at 44 h after plating using nanotemplate-assisted hanging vapor diffusion method. Images were taken at 12 successive time intervals while salt and protein crystals were sedimenting on the glass and the solution was evaporating. **A**: Total μGISAXS patterns of q_y versus q_z in A^{-1} unit, where, due to its high intensity, the specular peak is covered by a beamstop. **B**: Yoneda region of α_f dependency at $\alpha_i = 0.92$. In **panels** (**C** and **D**) are shown the projections along the center column with respect to the total μGISAXS scattering and the Yoneda regions, respectively.

salt and precipitant (Fig. 3C); in the Yoneda region of the buffer drop (Fig. 5C) three peaks do appear, with only the one with highest α_f being present before salt sedimentation but dominant and slightly off-axis after salt sedimentation.

- appears to change significantly along the z-axis and the y-axis whenever successively acquired at equally spaced time intervals over 7 min, at any time after plating either with the "classical" method [see the lysozyme data reported in Pechkova and Nicolini, 2005] or (mostly) with the protein nanotemplate-based method, apparently due to sedimentation processes of protein crystals from the solution (Fig. 2);
- along the z-axis changes from the very low q_z solution scattering of the total μGISAXS to the very low α_f protein substrate peak in the Yoneda region

For this reason in order to compare the crystallization process taking place with time in presence and absence of protein film as nanotemplate, we have kept constant the measuring time, carrying out the measurements quite rapidly immediately after removal from the container (Figs. 3–5). Under these conditions it appears that:

- the overall μGISAXS pattern of the drop containing P450scc crystallizing solution based on "nanotemplate" at 44 h after plating is quite more pronounced with respect to the corresponding "classical" one (Fig. 4).
- in the Yoneda region of the corresponding μGISAXS pattern, being the most sensitive to structural and morphological changes of the surfaces due to the interference effect involved in the occurrence of the Yoneda peak, contrary to "classical" drops "nanotemplate-based" P450scc cytochrome drops taken at 17 and 44 h after plating (Fig. 5) clearly show at least two pronounced Yoneda peaks growing with time after plating.

A week Yoneda peak exists already at shorter times with a critical angle corresponding to that

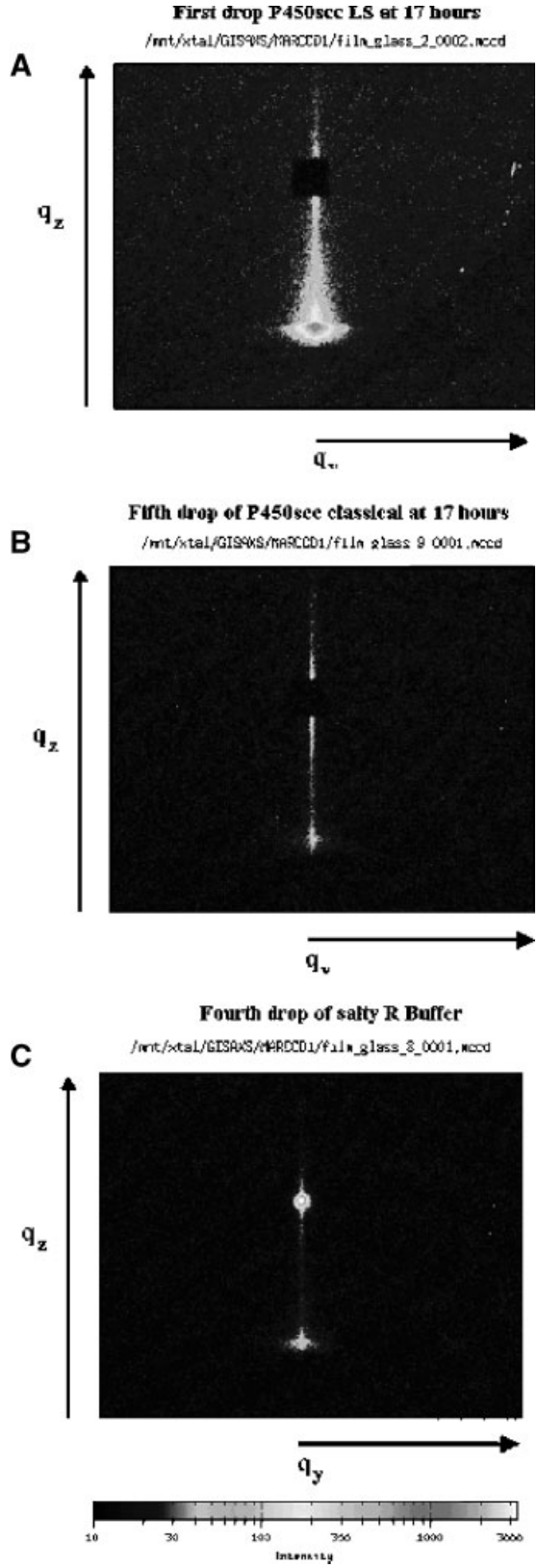

Fig. 3. Raw μGISAXS patterns of q_y versus q_z of three different drops deposited over ten layers of P450scc containing P450scc crystallizing solution at 17 h after plating either nanotemplate-based (**A**) or classical (**B**). The drop containing only the buffer solution with precipitant as described in the text is shown in (**C**).

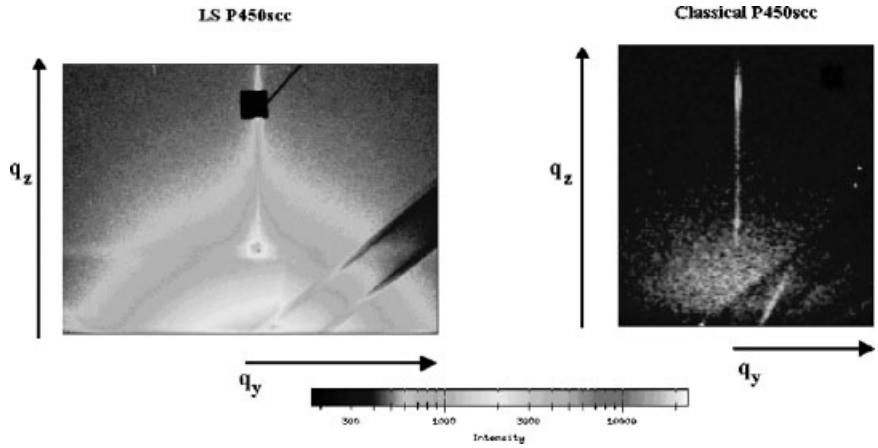

Fig. 4. The μGISAXS patterns of q_y versus q_z in drops containing P450scc crystallizing solution at 44 h after plating, either (**A**) ''nanotemplate-based'' over one monolayer P450scc, or (**B**) ''classical.''

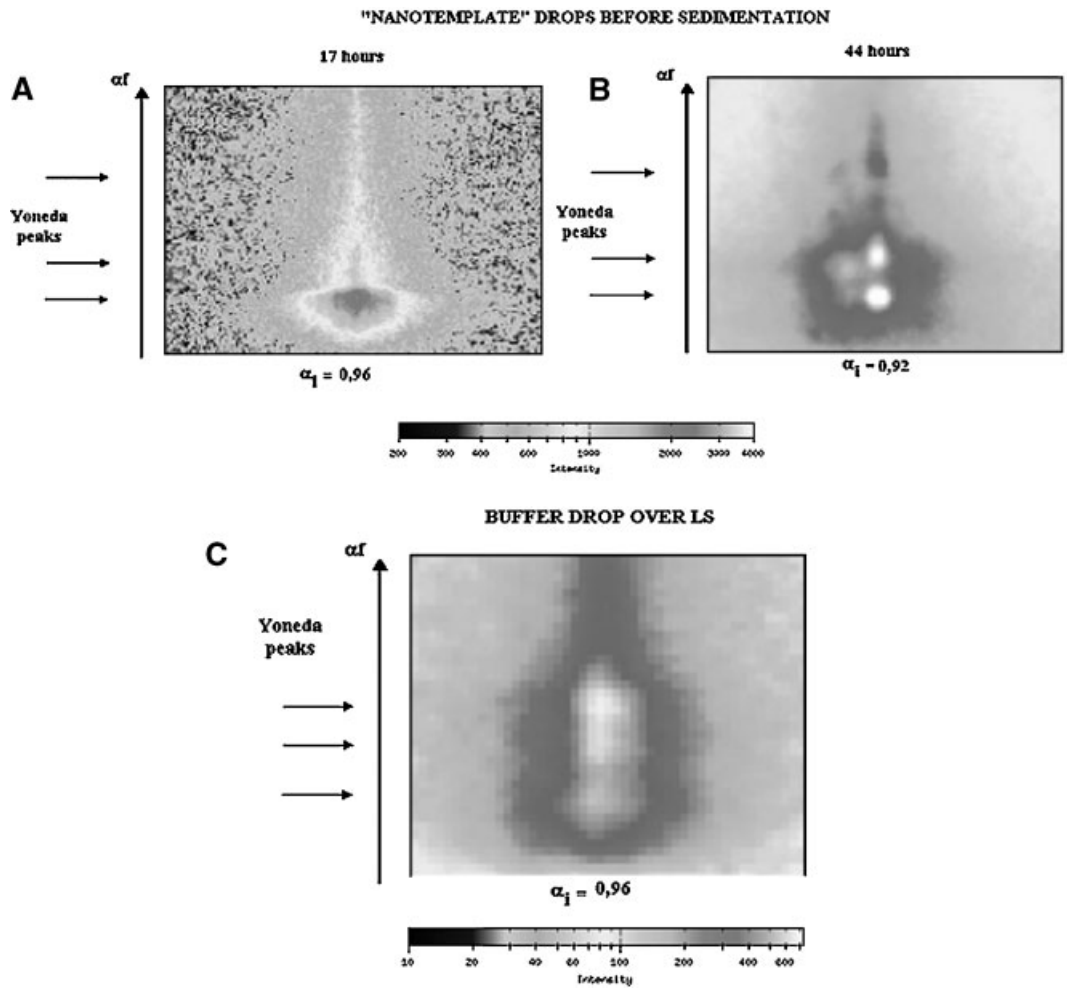

Fig. 5. Yoneda regions of P450scc cytochrome ''nanotemplate-based'' drops taken at 17 (**A**) and 44 h (**B**) after plating versus P450scc cytochrome, where the α_f dependency is given at $\alpha_i = 0.96$ and 0.92. Yoneda regions are indicated with arrows. The patterns are shown on a logarithmic scale to enhance the features in the Yoneda regions. With drops containing classical P450 crystallization solution or the buffer no significant signal is apparent under the same conditions with the acquisition being carried out immediately after drop deposition, After drop sedimentation with most liquid being evaporated a μGISAXS signal ten times less pronounced is apparent (see **panel C** for the corresponding buffer solution drop sitting on top of the same ten layers of P450scc). **Panel D** shows the projections in the LS drops with and without protein.

of the protein substrate, unlikely that of the salt precipitating on the substrate causing a new rough layer of small crystals, which yields a second peak not present at shorter times.

Hence all data are compatible with a working hypothesis, which attributes the peak at higher α_f-values to that of the glass substrate and/or to salt crystal with the newly developing peak at lower α_f-values being related to the protein itself.

Finally, in the attempt to obtain structural information at the atomic resolution we have then performed X-ray microdiffraction with the largest microcrystals (about 5 μm in diameter) being obtained by the homologous nanotemplate method after 44 h plating time in the form of "powder" P450scc microcrystals (Fig. 6B). A periodic structure of the P450scc cytochrome appears compatible with the diffracting rings present in Figure 6A. It is very difficult to analyze these preliminary data on the ultrasmall crystallite powder shown in Figure 6B. An attempt for indexing the diffraction pattern by radial averaging scattering function of the detector image scaled in q gave some periodicity at 4 and 11 Å.

CONCLUSIONS

The kinetics and the structure of the ultrasmall P450scc cytochrome microcrystals here investigated proves the superiority of the nanobiofilm template method [Pechkova and Nicolini, 2003, 2004] in inducing nucleation and growth up to a 5 μm crystal size of a protein system yet structurally unsolved. Our unprecedented approach with μGISAXS combines the powerful thin-film characterization method with the micrometer-sized X-ray beam enhancing the spatial resolution used thus far by two orders of magnitude [Roth et al., 2003; Pechkova et al., 2005]. The acquired scattering data (Figs. 2–5) along with the reproducible diffraction patterns of the ultrasmall P450scc microcrystals (Fig. 6) allows for a nondestructive and contact-free reconstruction of the crystallization process at the very early stage and of the three-dimensional structure and morphology of the nanocluster crystals. Such characterization and investigation on a submicrometric scale of extrasmall crystals cluster on top of the protein film appears to allow a more clear understanding of the very early steps of crystallization in P450scc cytochrome. It is worth to notice that even if these data are quite illuminating, more conclusive data will be likely obtained with the in-situ experimentation already being planned. The old study of Yoneda [1963] has been frequently cited, and the underlying models concerning surface roughness and the analytical interpretation of the diffuse scattering has been utilized to reach a conclusion. The proper models and conclusions were then decided by performing a zero-control experiment using a template with a droplet containing the solvent alone (no protein). Furthermore the influence of the surface coating on the scattering has been measured separately, including a control diffraction experiment with the surface coating alone. The available diffuse scattering data have also been interpreted compatibly with state-of-the-art knowledge.

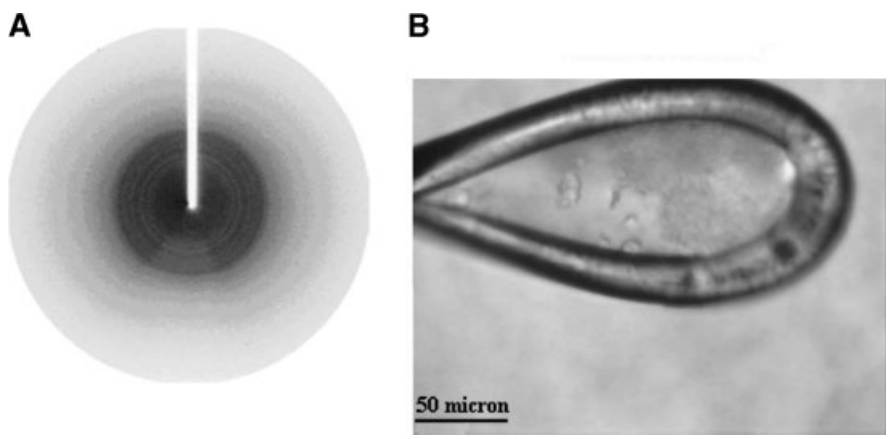

Fig. 6. Diffraction pattern of bovine P450scc ultramicrocrystal powder (**A**) apparently present in the microfocus loop (**B**) containing the P450scc drop at 44 h after the beginning of the crystallization process. The corresponding μGISAXS measurement is shown in Figure 4.

Considering that the Yoneda peak is one of the major informations extractable we have not made a simple generic comment, but pointed to the role of the density and of the roughness of the protein crystal and/or salt crystal layers. Detector scans are also shown in this context to interpreter the data where micro GISAXS pattern were provided and scaled to the same scattered intensity, taking into considerations the critical angles of the glass and of the proteins.

Interestingly, from the scattering data here obtained (Figs. 2–5) the occurrence and the time sequence of the various Yoneda peaks suggest the development of a layer with significant increase in roughness due to the significant increase in holes of the template layer as the P450scc crystal grows in the hanging drop. That is to say this model assumes a decreasing density of the protein template layer as the layer itself is removed by the protein solution thus triggering or assisting the formation of new crystals in the solution. In conclusion the data here presented favor a build-up of holes in the nanotemplate acting as nucleation centers for crystals formation in all protein systems including the ones so far impossible to crystallize as the human kinase [Pechkova and Nicolini, 2003; Pechkova et al., 2004] and the P450scc here studied.

ACKNOWLEDGMENTS

This work was supported by a FIRB-MIUR grant on Organic Nanosciences and Nanotechnology to the Nanoworld Institute, namely to the Fondazione EL.B.A and to the Centro Interuniversitario di Ricerca sulle Nanotecnologie e Nanoscienze Organiche e Biologiche of Genova University.

We are grateful to the cooperation of Christian Riekel, Manfred Burghammer and Stephan Roth of ESRF in acquiring the μGISAXS data at Grenoble.

REFERENCES

Ducruix A, Giege R. 1999. Crystallization of Nucleic Acids and Proteins. A Practical Approach. New York: Oxford University Press. pp 130–133.

Gehrke R. 1992. An ultrasmall angle scattering instrument for the DORIS-III bypass. Rev Sci Instrum 63:455–458.

Guinier A. 1963. X-ray diffraction in crystals, imperfect crystals and amorphous bodies. New York: Dover Publications, Inc.

Guinier A, Fournet G. 1955. Small angle scattering of X-rays. New York: John Wiley & Sons.

Holy V, Baumbach T. 1994. Nonspecular X-ray reflection from rough multilayers. Phys Rev B49:10668–10676.

Lazzari R. 2002. μGISAXS: A program for grazing-incidence small-angle X-ray scattering analysis of supported islands. J Appl Crystallogr 35:406–421.

Müller-Buschbaum P, Casagrande M, Gutmann J, Kuhlmann T, Stamm M, von Krosigk G, Lode U, Cunis S, Gehrke R. 1998. Determination of micrometer length scales with an X-ray reflection ultra small-angle scattering set-up. Europhys Lett 42:517–519.

Müller-Buschbaum P, Gutmann JS, Stamm M, Cubitt R, Cunis S, Von Krosigk G, Gehrke R, Petry W. 2000. Dewetting of thin polymer-blend films examined with GISAXS. Physica B 283:53–59.

Müller-Buschbaum P, Roth SV, Burghammer M, Diethert A, Panagiotou P, Riekel C. 2003. Multiple-scaled polymer surfaces investigated with micro-focus grazing incidence small-angle X-ray scattering. Europhysics Lett 61:639–645.

Nicolini C, Pechkova E. 2004. Nanocrystallography: An emerging technology for structural proteomics. Expert Review of Proteomics 1:253–256.

Pechkova E, Nicolini C. 2002a. From art to science in protein crystallization by means of thin film technology. Nanotechnology 13:460–464.

Pechkova E, Nicolini C. 2002b. Protein nucleation and crystallization by homologous protein thin film template. J Cell Biochemistry 85:243–251.

Pechkova E, Nicolini C. 2003. Atomic structure of a CK2α human kinase by microfocus diffraction of extra-small microcrystals grown with nanobiofilm template. J Cell Biochem 91:1010–1020.

Pechkova E, Nicolini C. 2004. Protein nanocrystallography: A new approach to structural proteomics. Trends in Biotechnology 22:117–122.

Pechkova E, Nicolini C. 2005. Structure and growth of ultrasmall protein microcrystals by synchrotron radiation: II. μGISAXS and Microscopy of Lysozyme. J Cell Biochem (in press).

Pechkova E, Tropiano G, Riekel C, Nicolini C. 2004. Radiation stability of protein crystals grown by nanostructured templates: Synchrotron microfocus analysis. Spectrochimica Acta B 59:1687–1693.

Pechkova E, Roth S, Burghammer M, Fontani D, Riekel C, Nicolini C. 2005. μGisaxs and protein nanotemplate crystallization: Methods and Instrumentation. J Synchrotron Rad (in press).

Riekel C. 2000. New avenues in X-ray microbeam experiments. Rep Prog Phys 63:233–262.

Roth V, Burghammer M, Riekel C, Müller-Buschbaum P, Diethert A, Panagiotou P, Walter H. 2003. Self-assembled gradient nanoparticle-polymer multilayers investigated by an advanced characterization method: Microbeam grazing incidence X-ray scattering. Appl Phys Lett 82:1935–1937.

Wada A, Mathew PA, Barnes HJ, Sanders D, Estabrook RW, Waterman MR. 1991. Expression of functional bovine cholesterol side chain cleavage cytochrome P450 (P450scc) in *Escherichia coli*. Arch Biochem Biophys 290:376–380.

Yoneda Y. 1963. Anomalous surface reflection of X-rays. Physical Review 161:2010–2013.